CHEMISTRY OF MATERIALS

VOLUME 17, NUMBER 22 NOVEMBER 1, 2005

Communications

Synthesis and Morphology of Star-Shaped Gold Nanoplates Protected by Poly(*N*-vinyl-2-pyrrolidone)

Mari Yamamoto,[†] Yukiyasu Kashiwagi,[†] Takao Sakata,[‡] Hirotaro Mori,[‡] and Masami Nakamoto[*,†]

Osaka Municipal Technical Research Institute, 6-50,
1-Chome, Morinomiya, Joto-ku, Osaka 536-8553, Japan, and
Research Center for Ultra-High Voltage Electron
Microscopy, Osaka University, Yamada-oka, Suita,
Osaka 565-0871, Japan

Received July 11, 2005
Revised Manuscript Received September 26, 2005

Finding a novel approach to architecturally controlled nanocrystal is a significant challenge toward future nanodevices because optical, electric, catalytic, and magnetic properties of nanocrystals extensively depend on their shapes and sizes.[1−3] Recently, the syntheses of metal and semiconductor nonspherical nanocrystals such as rod,[1,3−6] wire,[7] disk,[2,8−12] cubic,[13,14] and multipod[15−18] were carried out via the crystal growth in the isotropic liquid phase. On the other hand, the synthetic challenge for anisotropic gold nanoparticles has met with limited success since gold has a highly symmetric face-centered cubic (fcc) structure and usually tends to afford spherical shape to reduce its surface energy. Therefore, controlling the shape of gold nanocrystals requires utilization of a template such as surfactant or controlling growth condition and inducing techniques such as electrochemical method,[4] seeding growth approach,[5,15,17] and ultraviolet irradiation.[6] In fact, there exist a few strategies for preparing rod,[1,4−6] plate,[12] mono-/bi-/tri-/tetrapod,[15,16] and multipod.[17] To build up the nanocrystal with the desired shape, it is necessary to investigate the structural characterization and crystal growth processes for the shape determination.

Herein, we report the morphology of unprecedented star-shaped gold nanoplates and the crystal growth process in

---

[*] To whom correspondence should be addressed. E-mail: nakamoto@omtri.city.osaka.jp.

[†] Osaka Municipal Technical Research Institute.

[‡] Research Center for Ultra-High Voltage Electron Microscopy.

(1) Link, S.; El-Sayed, M. A. *J. Phys. Chem. B* **1999**, *103*, 8410.

(2) Jin, R.; Cao, Y.; Mirkin, C. A.; Kelley, K. L.; Schatz, G. C.; Zheng, J. G. *Science* **2001**, *294*, 1091.

(3) Peng, X.; Manna, L.; Yang, W.; Wickham, J.; Scher, E.; Kadavanich, A.; Alivisatos, A. P. *Nature* **2000**, *404*, 59.

(4) Yu, Y.-Y.; Chang, S.-S.; Lee, C.-L.; Wang, C. R. C. *J. Phys. Chem. B* **1997**, *101*, 6661.

(5) (a) Jana, N. R.; Gearheart, L.; Murphy, C. J. *J. Phys. Chem. B* **2001**, *105*, 4065. (b) Busbee, B. D.; Obare, S. O.; Murphy, C. J. *Adv. Mater.* **2003**, *15*, 414. (c) Nikhil, R. J. *Small* **2005**, *1*, 875.

(6) (a) Esumi, K.; Matsuhisa. K.; Torigoe, K. *Langmuir* **1995**, *11*, 3285. (b) Kim, F.; Song, J. H.; Yang, P. *J. Am. Chem. Soc.* **2002**, *124*, 14316.

(7) (a) Sun, Y.; Gates, B.; Mayers, B.; Xia, Y. *Nano Lett.* **2002**, *2*, 165. (b) Caswell, K. K.; Bender, C. M.; Murphy, C. J. *Nano Lett.* **2003**, *3*, 667.

(8) Puntes, V. F.; Zanchet, D.; Erdonmez, C. K.; Alivisatos, A. P. *J. Am. Chem. Soc.* **2002**, *124*, 12874.

(9) Maillard, M.; Giorgio, S.; Pileni, M.-P. *Adv. Mater.* **2002**, *14*, 1084.

(10) Germain, V.; Li, J.; Ingert, D.; Wang, Z. L.; Pileni, M.-P. *J. Phys. Chem. B* **2003**, *107*, 8717.

(11) Sun, Y.; Mayers, B.; Xia, Y. *Nano Lett.* **2003**, *3*, 675.

(12) (a) Malikova, N.; Pastoriza-Santos, I.; Schierhorn, M.; Kotov, N. A.; Liz-Marzán, L. M. *Langmuir* **2002**, *18*, 3694. (b) Ibano, D.; Yokota, Y.; Tominaga, T. *Chem. Lett.* **2003**, *32*, 574. (c) Shao, Y.; Jin, Y.; Dong, S. *Chem. Commun.* **2004**, 1104. (d) Millstone, J. E.; Park, S.; Shuford, K. L.; Qin, L.; Schatz, G. C.; Mirkin, C. A. *J. Am. Chem. Soc.* **2005**, *127*, 5312. (e) Porel, S.; Singh, S.; Radhakrishnan, T. P. *Chem. Commun.* **2005**, 2387.

(13) Ahmadi, T. S.; Wang, Z. L.; Green, T. C.; Henglein, A.; El-Sayed, M. A. *Science* **1996**, *272*, 1924.

(14) Sun, Y.; Xia, Y. *Science* **2002**, *298*, 2176.

(15) Chen, S.; Wang, Z. L.; Ballato, J.; Foulger, S. H.; Carroll, D. L. *J. Am. Chem. Soc.* **2003**, *125*, 16186.

(16) Hao, E.; Bailey, R. C.; Schatz, G. C.; Hupp, J. T.; Li, S. *Nano Lett.* **2004**, *4*, 327.

(17) Sau, T. K.; Murphy, C. J. *J. Am. Chem. Soc.* **2004**, *126*, 8648.

(18) Teng, X.; Yang, H. *Nano Lett.* **2005**, *5*, 885.

10.1021/cm0515000 CCC: $30.25

detail, where the star-shaped nanoplates have been prepared via the reduction of $HAuCl_4$ by L-ascorbic acid at room temperature in the presence of poly(*N*-vinyl-2-pyrrolidone) (PVP) with no use of Au seeds. Previous reports on gold nanoparticles with a star-shape prepared through the reduction of $HAuCl_4$ by L-ascorbic acid in the presence of silver nitrate, Au seeds, and cetyltrimethylammonium bromide (CTAB)[17] have not yet described their 3D shape, crystal structure, and growth directions of hones. With respect to the crystal structure of the star-shaped nanoparticles, only the PbS nanocrystal with six symmetric hones in the $\langle 100 \rangle$ directions, but not plates, has been reported to be synthesized at high temperature (180−250 °C) in organic solvent.[19] From the standpoint of the regulation of nanocrystals with desired shape, it is important to make clear both the detailed structure and the growing process of nanocrystals. This is the first report on the morphology and crystal growth of star-shaped gold nanoplates.

A typical procedure is as follows: 0.1 mL of an aqueous 20 mM $HAuCl_4 \cdot 4H_2O$ solution was added to 1 mL of aqueous 3 wt % PVP (average $M_w \approx 24500$) solution. Then, a freshly prepared 0.1 mL of an aqueous 40 mM solution of L-ascorbic acid (2 equiv to Au^{3+} ion) was added to the solution containing Au^{3+} ions and PVP at room temperature. The color of the resulting solution changed from pale yellow to colorless, suggesting the reduction of Au(III) to Au(I) species, and then the color of solution changed to red-purple within 5 min. The final pH was 2.3. The resulting solution was kept for 5 h at room temperature. To remove excess PVP and L-ascorbic acid, the following procedures were carried out one time: 10 mL of water was added to the reaction mixture, and then the resulting solution was centrifuged at 2000 rpm for 10 min. After centrifugation, 10 mL of the supernatant was discarded. It was confirmed that the UV−vis absorption spectrum of the sample obtained by this centrifugation at 2000 rpm for 10 min scarcely showed any change from that of the mother liquor before the centrifugation.

Figure 1 displays a TEM image of gold nanoparticles obtained by centrifugation at 2000 rpm for 10 min. Star-shaped nanoplates (~7%) and tripod or regular triangular plates (~4%) were observed among a large amount of spherical particles (~89%) including distorted or aggregated ones by counting 425 particles. However, it was substantially difficult to isolate the star-shaped nanoplates from other plates and the spherical nanoparticles by repeating centrifugation at 1000 rpm for 10 min. The average size of the star-shaped nanoplates obtained by measuring the length from a hone edge to another one on the opposite side became larger in the course of reaction by Ostwald ripening processes. For example, the average sizes of star-shaped nanoplates obtained by the reaction for 0.5, 2, and 5 h were 83 ± 13, 93 ± 18, and 95 ± 21 nm, respectively. On the other hand, the ratios of star-shaped nanoplates taken out after 0.5, 2, and 5 h were almost the same values (~7%).

To elucidate the 3D shape of the present star-shaped gold nanoplates, tilting experiments were performed, where the nanoplates should be held on a grid in a leaned arrangement against the incident electron beam because the sample holder could not tilt more than ±50°. Therefore, carbon nanotubes were utilized as supports for leaned nanoplates. The tilting experiments resulted in clear-cut TEM images, indicating that the particle is inherently a plate (Figure 2a−d). The thickness of the plate is estimated to be 25 nm from the side view of plate (Figure 2a).

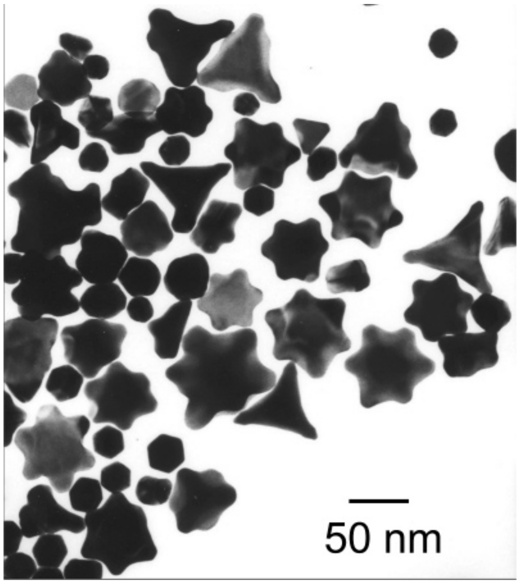

Figure 1. TEM image of gold nanoparticles.

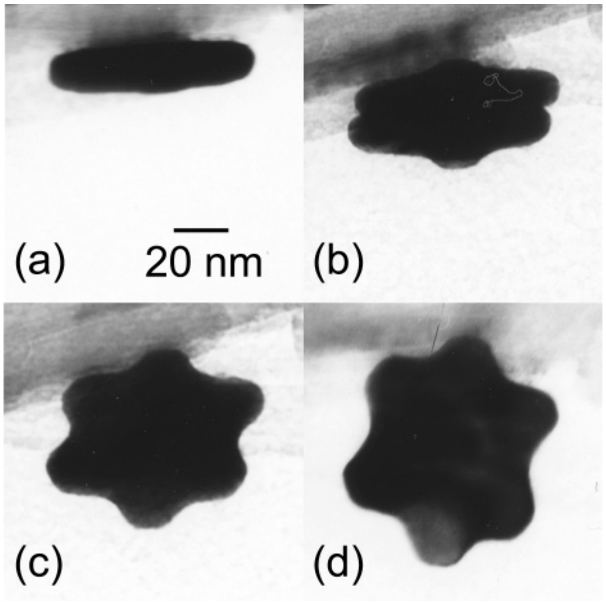

Figure 2. TEM images of a star-shaped nanoplate taken from different angles. The relative angles are (a) 0°, (b) 20°, (c) 45°, and (d) 83°.

The morphology of star-shaped nanoplates as shown in Figure 3a is attributed to their atomic structures. Figure 3b shows a selected area electron diffraction (SAED) pattern of the star-shaped nanoplate (Figure 3a) lying flat on the substrate. The SAED was taken with the incident electron beam perpendicular to the nanoplate face. The SAED pattern shows six sharp spots (boxed) corresponding to the {220} lattice planes with a 0.144 nm spacing of a face-centered cubic (fcc) crystal, indicating that the nanoplate face is parallel to {111}. Additional weak spots (triangle) corre-

---

[19] Lee, S.-M.; Jun, Y.-W.; Cho, S.-N.; Cheon, J. *J. Am. Chem. Soc.* **2002**, *124*, 11244.

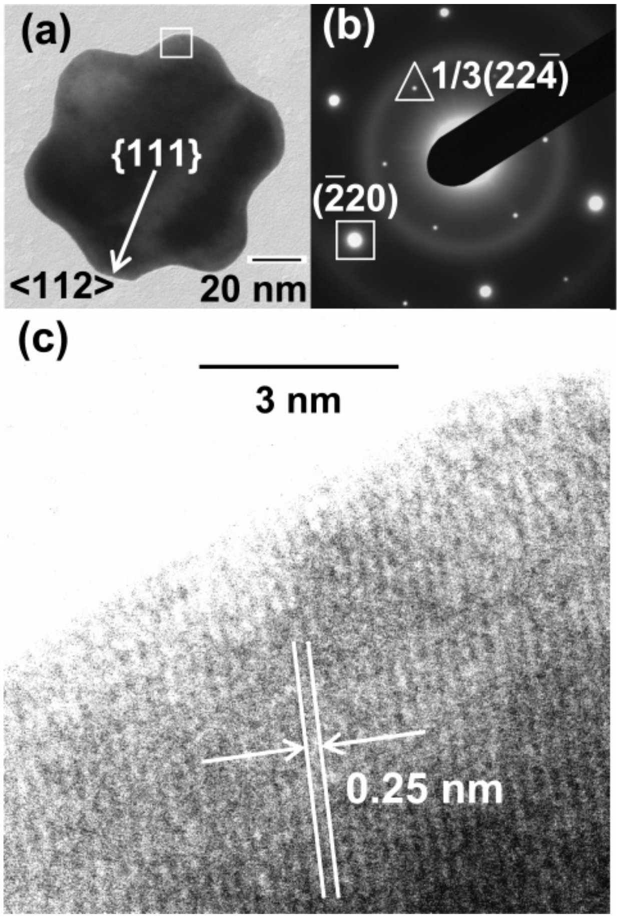

Figure 3. (a) TEM image of a regular star-shaped nanoplate. (b) Corresponding electron diffraction pattern taken with the incident beam perpendicular to the nanoplate face. The strong spots (boxed) could be indexed as the {220} diffractions, while the inner weaker spots (triangled) the forbidden 1/3{224} reflections. (c) HRTEM image of the edge of the nanoplate as marked by a white frame shown in panel a. The measured spacing of the fringes is three times the interplanar distance of {224}.

sponding to the forbidden 1/3{224} reflections with a 0.25 nm spacing were also observed. Such diffraction spots have been previously observed in plate-like Au and Ag nanocrystals.[2,9−11,12a,c] It is evident from a comparison of panels a with b of Figure 3 that each of the six hone grows in one of the ⟨112⟩ directions, suggesting that preferential hone growth occurred on the {112} planes. Figure 3c shows a high-resolution TEM (HRTEM) image of the nanoplate edge (Figure 3a) recorded from the ⟨111⟩ direction. The well-resolved interference fringe patterns also confirmed the single crystallinity of this gold nanoplate. The observed fringe spacing of 0.25 nm corresponds to the forbidden 1/3{224} reflection. These results shown in Figures 2 and 3 clearly indicate that the star-shaped nanoplates in this work are single-crystal nanoplates lying flat on their {111} planes with six symmetric hones extending to the ⟨112⟩ directions, but not the stacked two triangular plates or twin. To elucidate whether the growth directions of each hone change in the course of reaction, star-shaped nanoplates taken out at different reaction times (0.5, 2, and 5 h) were also measured by TEM and SAED. As a result, the preferential hone growth continuously proceeds on the {112} planes. In addition, the tripods found in Figure 1 also lay flat on their {111} planes and have hones with three ⟨112⟩ growth directions, confirmed by SAED and HRTEM techniques. These growth directions of hones are different from those of the Au[15] and Pt[18] tripods, which have {111} flat planes and three hones with the ⟨110⟩ growth directions. On the other hand, it has been reported that gold or silver nanoplates with triangular and hexagonal shapes have the flat top surface parallel to the {111} plane and the corners oriented to the ⟨112⟩ directions.[11,12b,c] In our case, the enhanced growth rate on the {112} faces of nanoplates with triangular and hexagonal shapes induces the extension of the three or six {112} branches into sharp triangular or star-shaped nanoplates.

The important factors in determining the morphology of the final product should be addressed as follows. (i) The high concentration of PVP more than 3 wt % is required for preparing star-shaped nanoplates. This suggests that nitrogen and oxygen atoms of the imide groups of PVP may function as a stabilizer coordinated on the {111} crystal faces. (ii) The equivalent amount of L-ascorbic acid to gold ions gave only hexagonal or triangular plates and spherical nanoparticles. The L-ascorbic acid may concern the enhanced growth on the {112} faces. (iii) The pH strongly affects the shape of nanoparticles.[5b] The final pH adjusted in the range from 2.7 to 2.0 by the addition of NaOH or HCl resulted in the production of star-shaped nanoplates. On the other hand, when the final pH adjusted by the addition of NaOH was 3.4 or 7.7, only spherical particles including distorted ones were produced. The induction period, when the color of solution changed from colorless to red-purple, became longer as the pH of the reaction mixture became much more acidic. This result is consistent with the reduction potential of L-ascorbic acid controlled by pH. Thus, the slow reduction of Au ions under the fairly acidic condition may result in the formation of star-shaped nanoplates.

In summary, we have investigated the morphology of well-defined star-shaped gold nanoplates and the crystal growth process in detail, where star-shaped nanoplates have been prepared by the simple method with no use of Au seeds: the reduction of $HAuCl_4$ by L-ascorbic acid in the presence of PVP under the ambient temperature. The various techniques of TEM have revealed that the star-shaped nanoplates were single crystal of flat plate with {111} face and six symmetric hones extending in the the ⟨112⟩ directions. The essential factors for the production of star-shaped nanoplates were the both amounts of PVP and L-ascorbic acid and pH control. Under the condition, the nuclear of star-shaped nanoplates are formed in the initial stage and then grow to the star-shaped nanoplates because their ratio does not change in the course of reaction. Thus, the addition of an appropriate nuclear as seed in the reaction solution may promote high yield preparation of star-shaped nanoplates.

CM0515000